# EFFECT OF MARANGONI CONVECTION GENERATED BY VOIDS ON SEGREGATION DURING LOW-G AND 1-G SOLIDIFICATION

M. Kassemi[1], A. Fripp[2], N. Rashidnia[1], and H. de Groh[3]

[1]NCMR, NASA GRC, Cleveland OH,
[2]NASA LaRC, Hampton, VA, [3] NASA GRC, Cleveland OH

## INTRODUCTION

Solidification experiments, especially microgravity solidification experiments, are often compromised by the evolution of unwanted voids or bubbles in the melt. Although these voids and/or bubbles are highly undesirable, there is currently no effective means of preventing their formation or of eliminating their adverse effects, particularly during microgravity experiments. Marangoni convection caused by these voids can drastically change the transport processes in the melt. Recent microgravity experiments by Matthiesen (1) , Andrews (2) and Fripp (3) are perfect examples of how voids and bubbles can affect the outcome of costly space experiments and significantly increase the level of difficulty in interpreting their results.

Formation of bubbles have caused problems in microgravity experiments for a long time. Even in the early Skylab mission an unexpectedly large number of bubbles were detected in the four materials processing experiments reported by Papazian and Wilcox (4). They demonstrated that while during ground-based tests bubbles were seen to detach from the interface easily and float to the top of the melt, in low-gravity tests no detachment from the interface occurred and large voids were grown in the crystal. More recently, the lead-tin-telluride crystal growth experiment of Fripp *et al.*(3) flown aboard the USMP-3 mission has provided very interesting results. The purpose of the study was to investigate the effect of natural convection on the solidification process by growing the samples at different orientations with respect to the gravitational field. Large pores and voids were found in the three solid crystal samples processed in space. Post-growth characterization of the compositional profiles of the cells indicated considerable levels of mixing even in the sample grown in the hot-on-top *stable* configuration. The mixing was attributed to thermocapillary convection caused by the voids and bubbles which evolved during growth. Since the thermocapillary convection is orientation-independent, diffusion-controlled growth was not possible in *any* of the samples, even the top-heated one. These results are consistent with recent studies of thermocapillary convection generated by a bubble on a heated surface undertaken by Kassemi and Rashidnia (5-7) where it is numerically and experimentally shown that the thermocapillary flow generated by a bubble in a *model* fluid (silicone oil) can drastically modify the temperature field through vigorous mixing of the fluid around it, especially under microgravity conditions.

In the present research effort we investigate both numerically and experimentally the effect of thermocapillary convection generated by a void/bubble on the growth of a typical single crystal alloy. In this paper, we only present some of the microgravity numerical simulations to demonstrate in detail the manner in which the void-generated convection can modify the temperature stratifica-

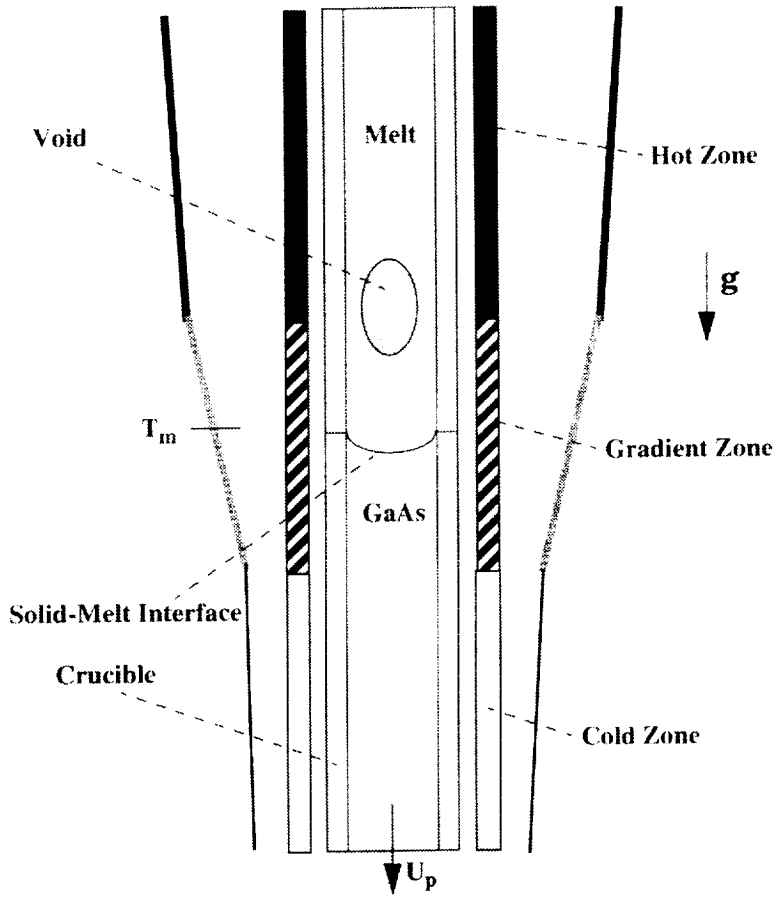


Figure 1. Schematic of the Bridgman Growth Configuration.

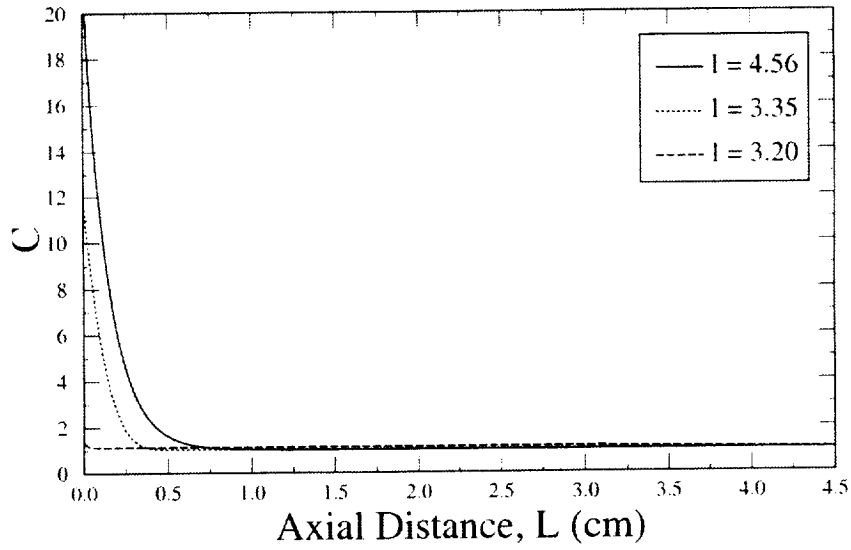


Figure 2. Concentration along the central axis of symmetry for different void-interface distance, *l*(cm).

tion and the segregation patterns in the dilute binary melt during various stages of a microgravity solidification experiment. These results characterize and quantify for the first time the serious impact of voids and/or bubbles on the growth of single crystal in space. The ground-based SCN experiments and the associated numerical simulations will be covered in future papers and reports.

## I. Results and Discussion

Consider the growth of a single crystal (in this case selenium-doped GaAs) from a dilute two-component melt in a vertical Bridgman furnace as depicted in Figure 1. The ampoule is placed in a three- zone furnace which consists of fixed hot and cold zones separated by a sharp gradient region. Directional solidification takes place as the ampoule is translated at a constant rate. The transport of heat among the solid, the melt, the ampoule, and the furnace determines the solid-melt interface shape and position. The numerical simulations presented here correspond to a situation where a void is present in the melt. The quasi-steady simulations show the effect of the thermocapillary convection generated by the void on the temperature and concentration fields in the melt at different stages of the solidification process as the distance between the solid-melt inter-face and the void is reduced.

The first case examined corresponds to the initial stages of the solidification process where there is a relatively large distance between the growth interface and the void ($l = 4.56$ cm). The axial concentration profile (at the center of the ampoule) for this case is presented in Figure 2 and the temperature, concentration, and flow fields are presented in Figure 3. In this situation, the void is in the shallow gradient region (hot zone) of the ampoule. Nevertheless a thermocapillary vortex is generated in the vicinity of the bubble as shown in Figure 3a. The vortex recirculates the fluid along the void interface in a clockwise direction. The flow is not too strong and is restricted to the mostly uniform temperature and concentration regions of the ampoule, therefore, it does not affect the melt temperature and concentration fields appreciably. The concentration and velocity profiles along the axis of symmetry (ampoule centerline) are presented in Figures 2 and 4, respectively. The solutal boundary layer at the growth interface is very thin and extends only about 0.75cm into the melt as depicted in Figure 2. The velocity boundary layers around the void are shown in Figure 4 for several different void-interface locations. Note that for the $l = 4.56$ *cm* case, the flow dies long before it can penetrate the solutal boundary layer. As a result at $l = 4.56$ cm, the solidification process is unaffected by the void-generated convection. The radial concentration profile along the growth interface for this case and several other void-interface distances are included in Figure 5. The $l = 4.56$ *cm* concentration profile is parabolic at the melt-solid interface with the maximum dopant concentration occurring in the middle of the interface. This indicates an appreciable amount of radial segregation, which is mainly caused by the interface curvature.

The interfacial segregation pattern changes drastically as shown in Figure 5 when the void-interface distance, l, is reduced. This can be explained by examining the flow and concentration fields of the $l = 3.2$ *cm* case, for example, as included in Figure 6a. In this case, the thermocapillary vortex shown in Figure 6a has penetrated the solutal build-up region near the growth interface. This is corroborated by an examination of the velocity profile along the ampoule centerline in Figure 4 which shows that the velocity boundary layer for this case extends all the way to the growth interface. The strong thermocapillary vortex nearly wipes out the solute boundary layer at the growth interface as indicated by the concentration field in Figure 6a and homogenizes the dopant concentration throughout the ampoule through vigorous mixing. The $l = 3.2$ *cm* axial and radial concentration profiles included in Figures 2 and 5a are both indicative of an almost fully-mixed regime. But a closer look at the radial segregation pattern on an expanded scale as shown in Figure 5b still indicates a noticeable nonuniformity in the interfacial concentration profile. The thermocapillary mixing effect becomes more pronounced as the void and the interface get closer to each other. At $l = 1.95$ *cm* the void is in the high temperature gradient region. Consequently, the thermocapillary flow intensifies with an almost five-fold increase in the maximum velocity as shown in Figure 4. This creates a substantial amount of mixing near the interface as indicated by the concentration and flow fields in Figure 6b which produces an even more uniform concentration profile at the growth interface.

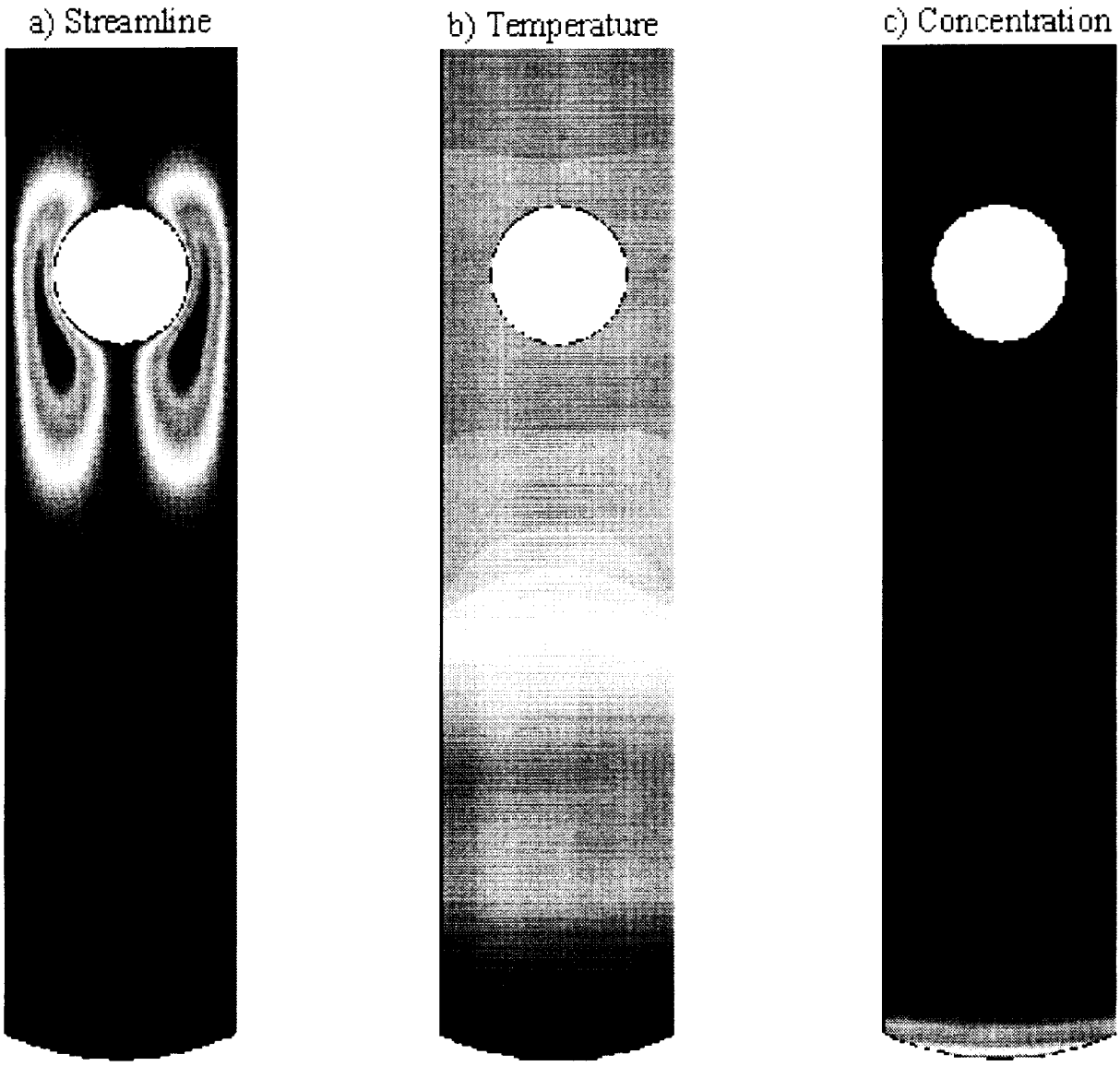


Figure 3. Streamline (a), Temperature (b), and Scaled Concentration (c) fields for $l$=4.56cm case.

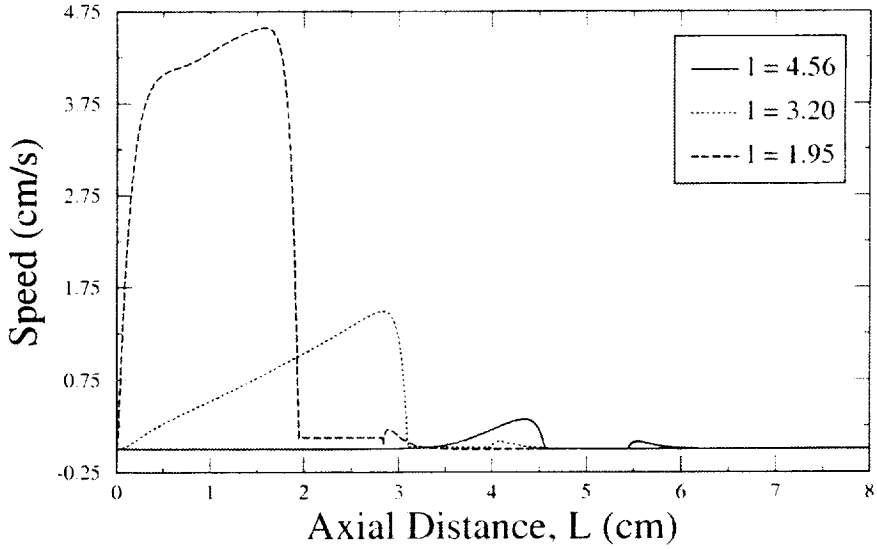


Figure 4. Speed along the central axis of symmetry for different void-interface distances, $l$(cm).

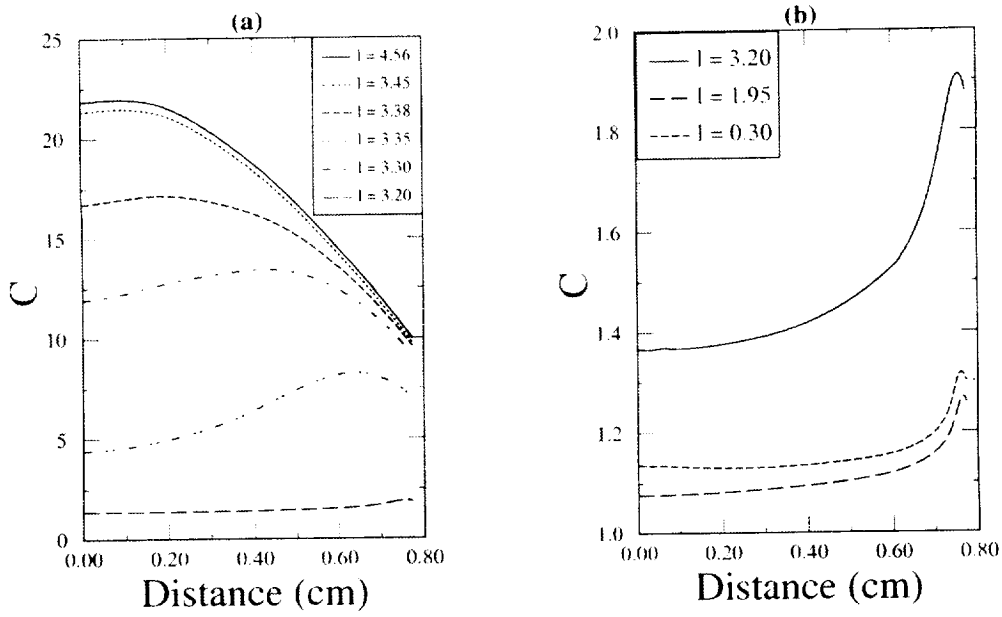


Figure 5. Concentration along the solid-melt interface for different void-interface distances $l$ (cm).

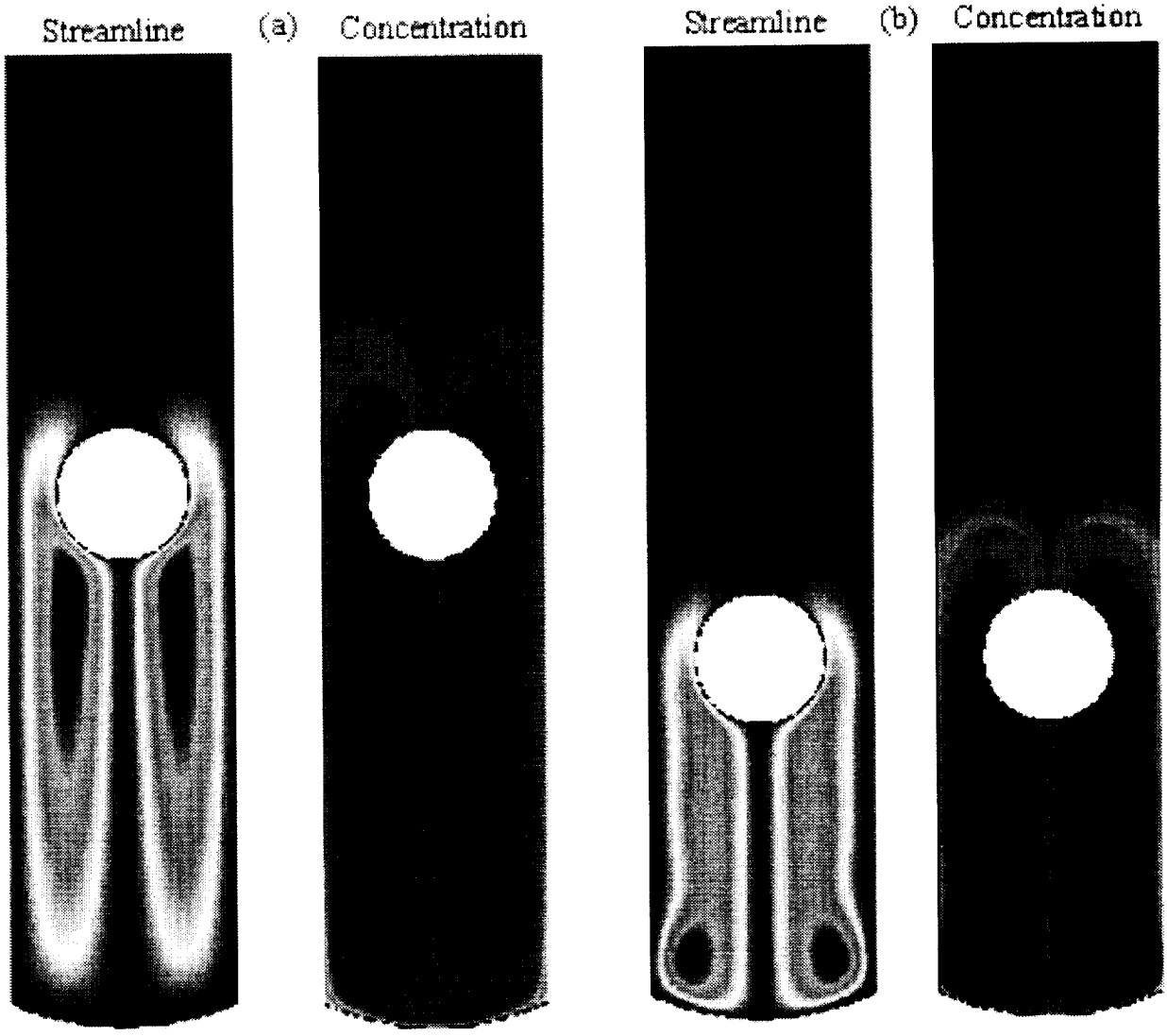


Figure 6. Streamline and scaled concentration fields for $l$=3.20 cm (a) and $l$ =1.95 cm (b) cases.

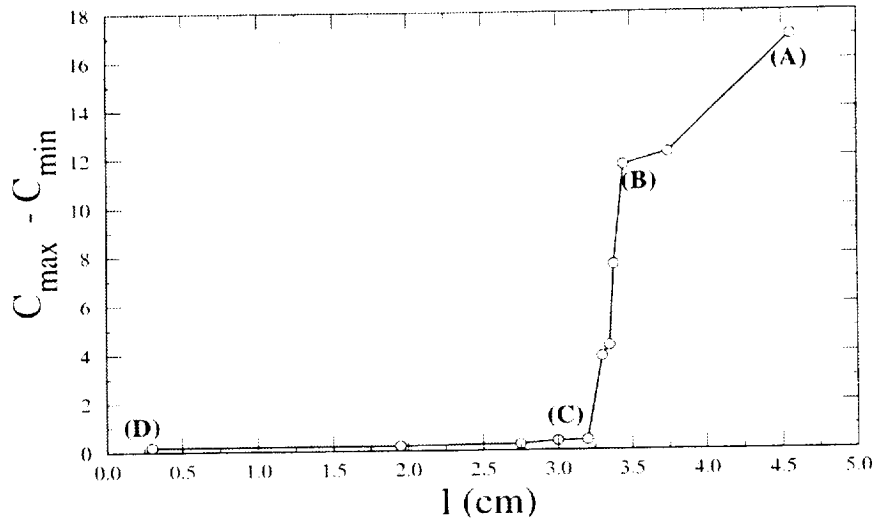


Figure 7. Plot of radial segregation versus void-interface distance.

## II. Conclusion

The results of this analysis can be succinctly summarized by plotting the magnitude of the radial segregation against the void-interface distance as shown in Figure 7. From a transport point of view, there are three distinct regions on this plot. Points (A) to (B) correspond to the region where the solutal boundary layer is minimally affected by the void-generated thermocapillary convection. The segregation behavior in this region is dominated by diffusion and is caused almost entirely by the interface curvature. Points (B) to (C) designate a region where the thermocapillary flow begins to influence the segregation pattern considerably (see Figure 5a) but has not yet penetrated the solutal boundary layer at the growth interface. In this region the extent of the radial segregation and the distribution of the interfacial composition change drastically with small variations in the void-interface distance. Finally, the segment bounded by points (C) to (D) correspond to the region where the vigorous thermocapillary flow wipes out the solutal boundary layer and a fully-mixed regime is approached.

## REFERENCES


1. Matthiesen D.H., and Majewski, J.A., *The Study of Dopant Segregation Behavior During the Growth of GaAs in Microgravity*, In Joint Launch + One Year Review of USML-1 and USMP-1, NASA CP 3272, Vol1, p223, May 1994.
2. Andrews, J. B., Hayes, L.J., Arikawa, Y., and, Coriell, S.R., *Microgravity Solidification of Al-In Alloys*, AIAA 97-1012, 1997.
3. Fripp, A.L., and et al., *The Effect of Microgravity Direction on the Growth of PbSnTe*, AIAA 97-0676, 1997.
4. Papazian, J. M. and Wilcox, W. R., *Interaction of Bubbles with Solidification Interfaces*, AIAA J., Vol. 16, 447- 451, 1978.
5. Kassemi, M., and Rashidnia, N., *Steady and Oscillatory Thermocapillary Flows Generated by a Bubble in 1-G and Low-G Environments*, AIAA 97-0924, presented in the 35th AIAA Aerospace Conference, 1997.
6. Kassemi. M., Rashidnia, N. and Mercer, C., *Numerical and Experimental Visualization of Oscillatory Temperature and Velocity Fields Generated by a Bubble*, Proceedings of The 8th International Symposium in Flow Visualization, Eds. G.M. Carlomagno and I. Grant, pp. 284.1-284.11, 1998